Brain Tumor Segmentation: a comparative analysis of traditional Image Processing techniques, investigating a novel threshold algorithm versus Otsu

Mattia Tritto

Department of Electrical and Information Engineering at Politecnico di Bari

---

Abstract

With the rising significance of medical imaging in cancer diagnosis, Magnetic Resonance Imaging (MRI) has emerged as a pivotal tool for detecting brain tumors. This report tests an approach proposed by Ilhan U., & Ilhan A. [3] aimed at distinctly delineating cancer-affected tissues. Furthermore, this report discusses modifications to the preprocessing and post-processing steps, wherein various reasonable approaches were tested and the one yielding the best performance was selected. The primary objective is to provide doctors clear, detailed observations for improved tumor diagnosis. Comparative analysis reveals that the proposed methodology outperforms existing approaches like Otsu, presenting a more effective and precise solution for brain tumor segmentation.

Introduction to brain tumors and different types of MRI images

Tumor is an uncontrolled growth of cancer cells in any part of the body. Tumors are of different types and have different characteristics and different treatments. At present, brain tumors are classified as **primary brain tumors** and **metastatic brain tumors**. The former begin in the brain and tend to stay in the brain, the latter begin as a cancer elsewhere in the body and spreading to the brain.

Brain tumors are divided into two types: **benign** and **malignant**. In fact, the most widely used grading scheme has been issued by the *World Health Organization* (WHO)[1]. It classifies brain tumors into grade **I to IV**. In general, grade I and grade II are benign brain tumor (low-grade); grade III and grade IV are malignant brain tumor (high-grade). Usually, if low-grade brain tumor is not treated, it is likely to deteriorate to high-grade brain tumor. Therefore, brain tumor are seriously endangering people's lives and early discovery and treatment have become a necessity. In the clinical aspect, treatment options for brain tumor include surgery, radiation therapy or chemotherapy.

Along with the advance of medical imaging, imaging modalities play an important role in the evaluation of patients with brain tumors and have a significant impact on patient care. Recent years, the emerging new imaging modalities, such as *X-Ray*, *Ultrasonography*, *Computed Tomography* (CT), *Magneto Encephalo Graphy* (MEG), *Electro Encephalo Graphy* (EEG), *Positron Emission Tomography* (PET), *Single-Photon Emission Computed Tomography* (SPECT), and *Magnetic Resonance Imaging* (MRI), not only show the detailed and complete aspects of brain tumors, but also improve clinical doctors to study the mechanism of brain tumors at the aim of better treatment. Therefore, the evaluation of brain tumors with imaging modalities is now one of the key issues of radiology departments. **MRI is a non-invasive and good soft tissue contrast imaging modality, which provides invaluable information about shape, size, and localization of brain tumors without exposing the patient to a high ionization radiation** [2]. MRI is attracting more and more attentions for the brain tumor diagnosis in the clinical. In current clinical routine, the images of different MRI sequences are employed for the diagnosis and delineation of tumor compartments. These sequence images include *T1-weighted MRI* (**T1w**), *T1-weighted with gadolinium contrast MRI* (**T1gd**), *T2-weighted MRI* (**T2w**), *FLuid-Attenuated Inversion Recovery* (**FLAIR**), etc. *Figure 1* shows an horizontal slice of the four standard sequences for a tumor:

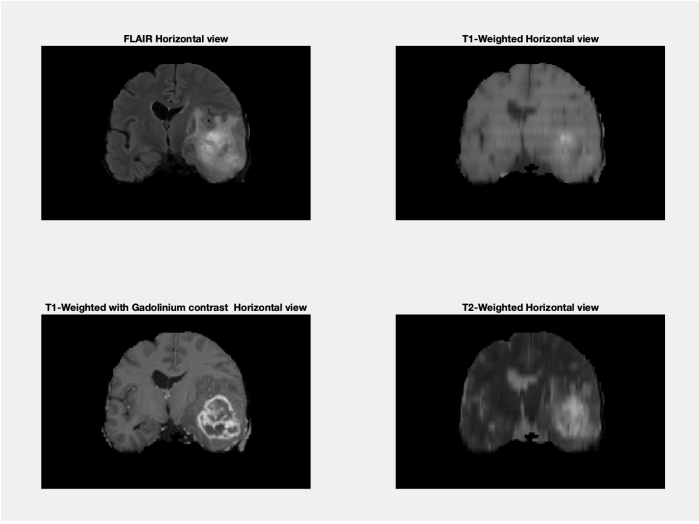

Figure 1: (FLAIR, T1w, T1gd, T2w MRIs)

T1-gd sequence images can make the brain tumor borders become brighter because the contrast agent accumulates there due to the disruption of the blood-brain barrier in the proliferative brain tumor region. In these sequence images, the necrotic core and the active cell region can be distinguished easily (*Figure 2*).
In T2w, the edema region can appear brighter than other sequence images of MRI. Since the signal of water molecules is suppressed in the imaging process of FLAIR, FLAIR is regarded as a highly effective sequence image to help separate the edema region from the CSF.

Due to the large amount of brain tumor images that are currently being generated in the clinics, it is not possible for clinicians to manually annotate and segment these images in a reasonable time. Hence, the automatic segmentation has become inevitable. Brain tumor segmentation is to segment abnormal tissues such as active cells, necrotic core, and edema from normal brain tissues including GM, WM, and CSF.¶

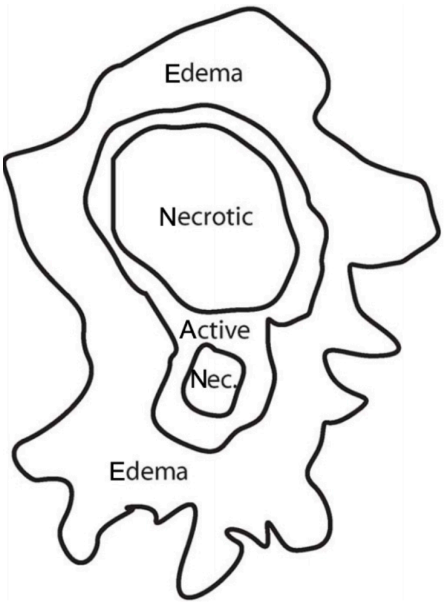

Figure 2: necrotic core, active cell region and edema

Literature review

In the world of image processing and segmentation, there are several techniques to segment brain tumors.

Thresholding algorithms constitute a fundamental approach whereby pixels in an image are partitioned into foreground and background based on their intensity levels relative to a specified threshold value. These algorithms are characterized by their simplicity and efficiency, making them suitable for various applications where clear intensity disparities exist between objects and background regions. [3] is the one that is used in this report.

Contour-based algorithms, on the other hand, leverage the concept of delineating object boundaries through the extraction of continuous curves or contours that encapsulate the desired objects. These algorithms focus on identifying transitions in intensity or color gradients within the image to delineate object boundaries accurately [4].

Lastly, the utilization of **K-means clustering** presents an alternative approach wherein pixels are grouped into clusters based on their feature similarity, often in terms of intensity values. K-means clustering facilitates the partitioning of an image into distinct regions or classes, allowing for the segmentation of objects based on their inherent features rather than explicit thresholding. Each of these techniques contributes distinct advantages and capabilities to the field of image segmentation, catering to diverse application scenarios and image characteristics [5].

Dataset used

The data set consists of 750 multiparametric-magnetic resonance images (mp-MRI) from patients diagnosed with either glioblastoma or lower-grade glioma. The sequences used were native T1-weighted (T1), post-Gadolinium (Gd) contrast T1-weighted (T1-Gd), native T2-weighted (T2), and T2 Fluid-Attenuated Inversion Recovery (FLAIR). The corresponding target ROIs were the three tumor sub-regions, namely edema, enhancing, and non-enhancing tumor. The Brain data set contains the same cases as the 2016 and 2017 Brain Tumor Segmentation (BraTS) challenges [6].¶

Segmentation steps

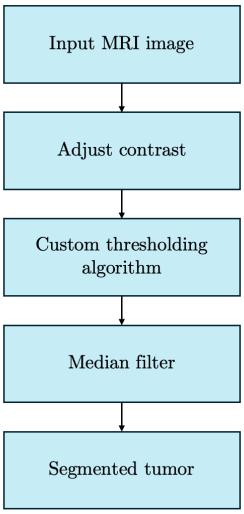

Figure 3: a brief summary of the stages used for segment the tumor

1. For the preprocessing stage, it was involved a function for **adjusting the contrast** of the input brain MRI image. You achieve this by examining the histogram of the image and expanding its intensity range based on what the histogram tells you. This process helps to **enhance the visual quality of the image** and improve slightly the accuracy of subsequent processing steps.

2. **Segmentation using the proposed thresholding algorithm**: in this method, sum of unique pixel values excluding zeros (black pixels) are divided by the count of unique pixel values. By this operation, the average gray value (threshold value) is calculated to convert the grayscale image to binary image

3. After obtaining the binary segmented image, I applied a **median filter**. The median filter helps in reducing noise in the form of "salt and pepper" of the segmented regions, resulting in a more refined segmentation output. The median filter is the most commonly used non-linear filter. In this filter, the median pixel value in the neighbourhood is calculated and the middle pixel value in the neighbourhood is replaced by the calculated median pixel value. While calculating the median pixel value, all the pixel values in the neighbourhood are first sorted in ascending order, and then the median pixel is the one used to substitute the center pixel.

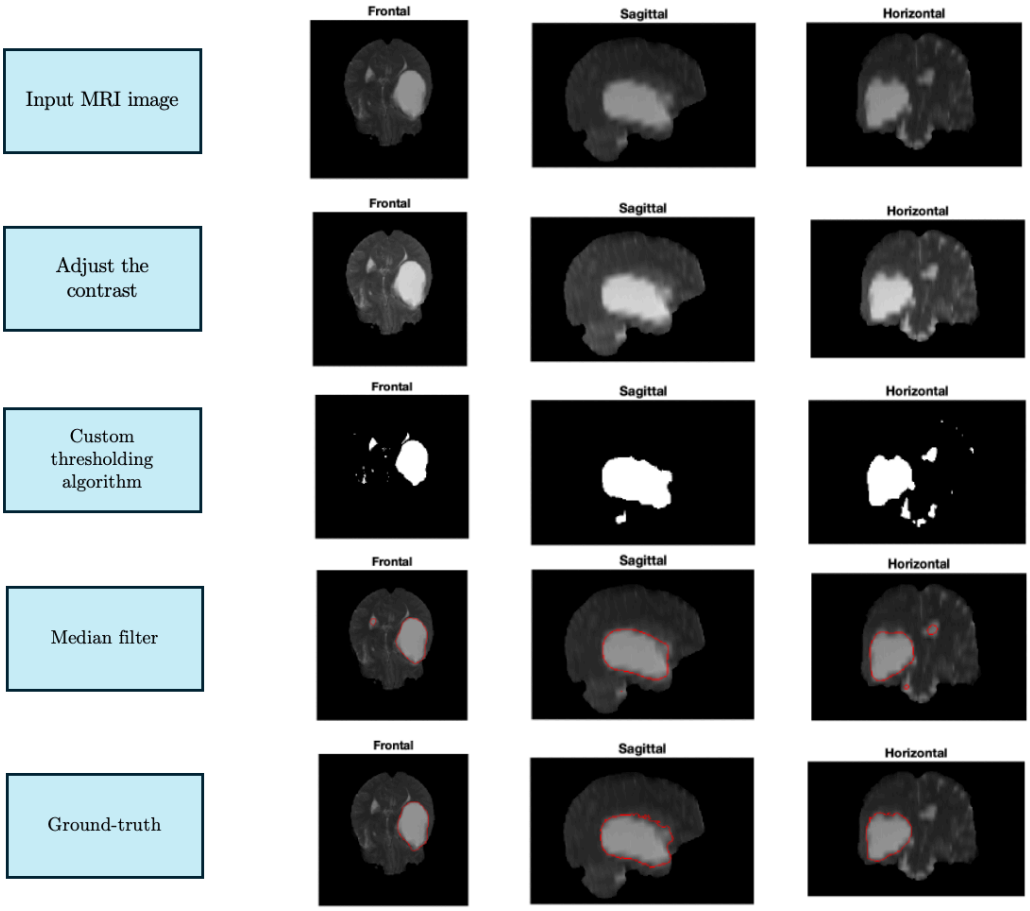

Figure 4: example of segmentation on one of the best performing images from the BRATS dataset

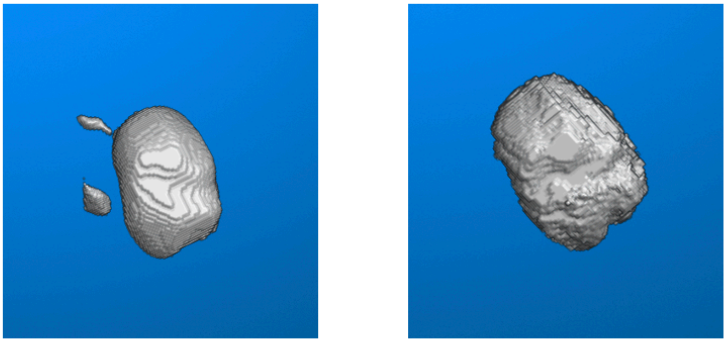

Figure 5: on the left the 3D segmented tumor, on the right the ground-truth tumor

Evaluation and fine tuning process

To quantify in an objective way the goodness of the segmentation process, I used these 4 metrics: **accuracy**, **DICE**, **Intersection over Union** (IoU) and the **difference of volumes between ground-truth and segmented tumor**.

Accuracy is a measure of the overall correctness of the segmentation, calculated as the ratio of correctly classified pixels to the total number of pixels in the image.

Dice coefficient quantifies the overlap between the segmented region and the ground truth region, calculated as twice the intersection of the segmented and ground truth regions divided by the sum of their areas. A Dice coefficient of 1 indicates perfect overlap, while 0 indicates no overlap.

Intersection over Union (IoU), also known as the Jaccard Index, measures the similarity between the segmented and ground truth regions, calculated as the ratio of the intersection area to the union area of the two regions. IoU ranges from 0 to 1, where 1 indicates perfect overlap and 0 indicates no overlap.

Regarding the fine-tuning process, my first mission was to figure out **which of the four images would be the best for this particular segmentation technique**. To do that, I checked out the four different metrics mentioned before. Here's what I found:

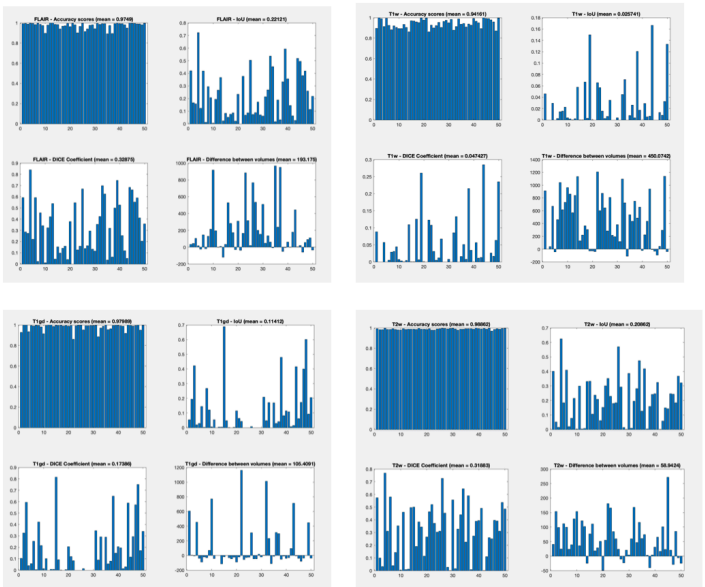

Figure 6: comparison between the four MRI imaging modalities given

The first observation we can extract from these bar plots is that, as expected, this algorithm tends to **suffer from under-segmentation** (as indicated by the positive difference volume in most of the cases). Here's the chain of thoughts I followed for choosing the right image. First off, T1-w consistently scored the lowest in all four metrics, so it was quickly ruled out. Given that this is a threshold algorithm and not a contour-based one, T1-gd isn't the ideal choice in this scenario. This is because it primarily highlights the edges rather than the entire tumor area. Ultimately, **I decided to go with T2w** over FLAIR images because it exhibits significantly less over-segmentation, as evidenced by the difference in volumes.

The second goal was to find the **best parameters for the median filter and for the image contrast stretching functions**, so I treated the upper bound for contrast stretching and the dimensions of the median kernel filter as variables to fine-tune, aiming to obtain the optimal values for them. Therefore, *test2.m* iterated over various combinations of these parameters and selected reasonable values for the upper contrast stretching and the dimensions of the median filter kernel. Subsequently, I plotted an heatmap for each metric used to determine the best-performing combination of parameters:

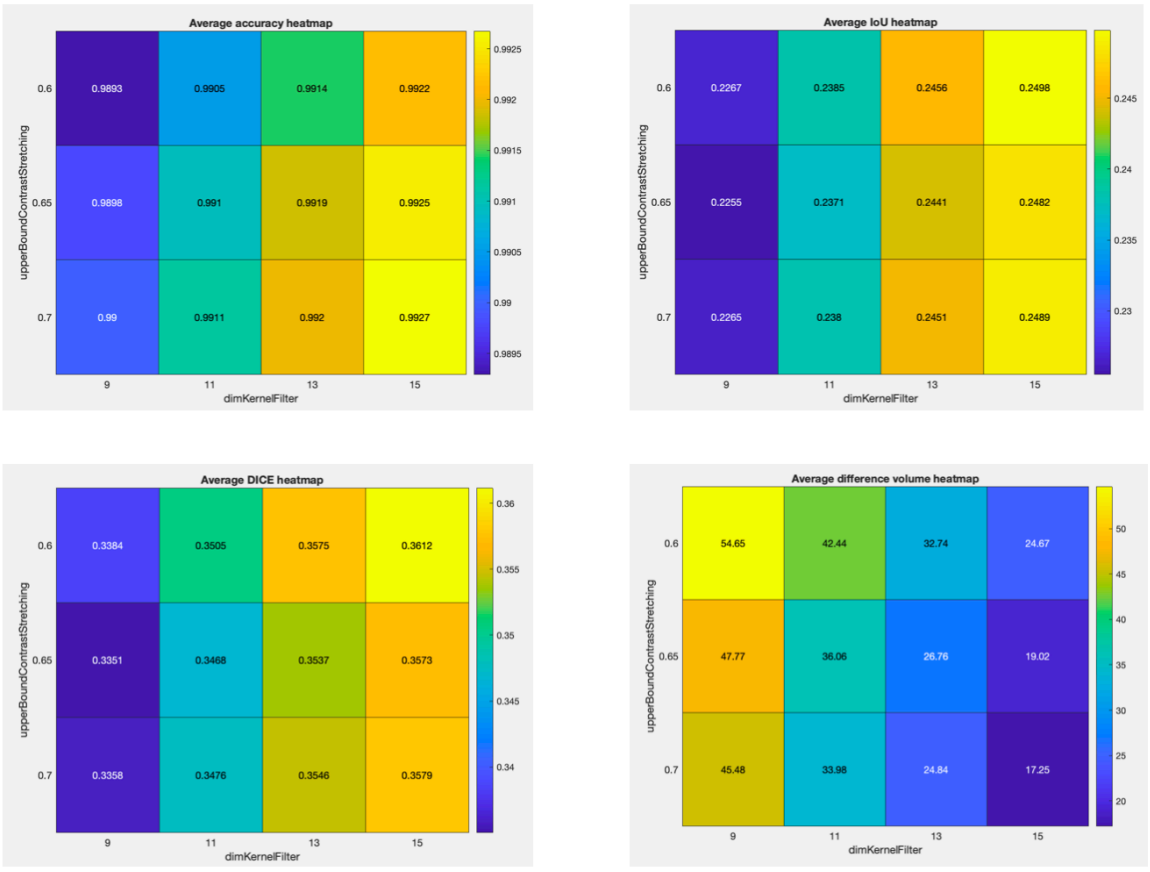

Figure 7: fine-tuning heatmaps to determine the best performing parameters

As observed, the **kernel dimension appears to be the primary driver influencing all four metrics**. Based on the heatmap analysis, I opted for a **kernel dimension of 15**. Conversely, the specific value of the upper limit for contrast stretching seems to have minimal impact. Therefore, I selected **0.7 as the optimal choice,** as it resulted in the least discrepancy between the volume of the segmented tumor and the label given.

In the end, after fine-tuning the parameters of our custom thresholding segmentation algorithm, I **compared this custom thresholding approach with the standard Otsu algorithm**. The Otsu algorithm is commonly used in various applications for finding a threshold value for binarizing images. Here are the results of the comparison:

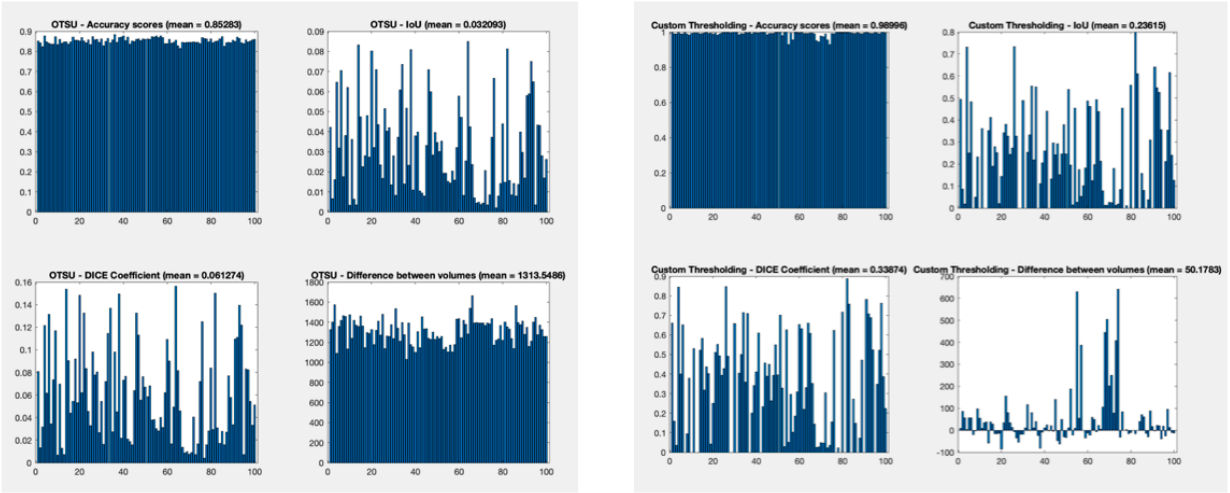

Figure 8: comparison between custom thresholding algorithm VS Otsu

Upon reviewing these bar plots, it's evident that **custom thresholding outperforms Otsu thresholding across all metrics**. However, to be honest, this comparison may not be entirely fair. In paper [3], only accuracy was mentioned, which can be misleading as it tends to yield higher values anyway. When considering more appropriate metrics such as IoU or DICE coefficient, it becomes clear that the Otsu method yields nearly zero values. This indicates that **Otsu fails completely to segment tumors**, which is noticeable also by inspecting the resulting segmentation visually:

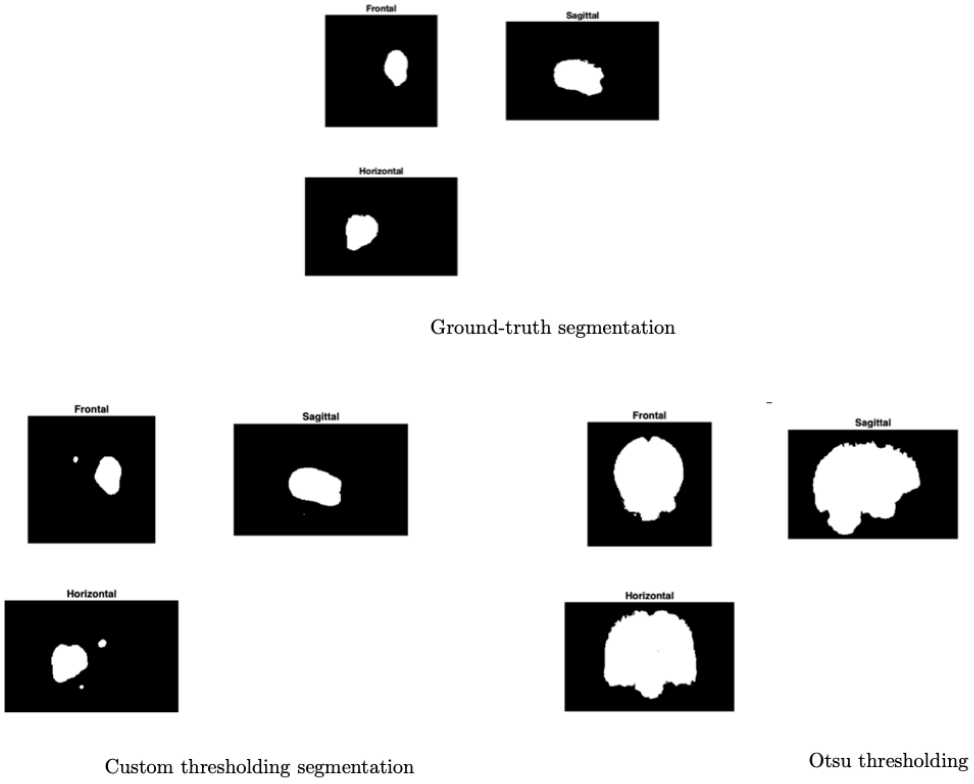

Figure 9: comparison between custom thresholding algorithm VS Otsu

In addition, I attempted to incorporate preprocessing steps before the segmentation by applying an **image sharpener like a 3D Laplacian filter** [7]. However, the results did not align with the benchmark obtained before. All four performance metrics were lower compared to when this stage was omitted, so this option was discarded. An explanation for this is that since this is not a counter-based algorithm, sharpening the image is not useful in this case.

A similar attempt was made using an **average filter**, to explore whether applying a low pass filter before the segmentation step could yield improved results. However, the outcome mirrored the previous attempt.

Conclusions

The custom thresholding algorithm produces **acceptable results** in terms of **detecting the tumor's location**, although it **suffers from under-segmentation issues**.

While traditional image processing algorithms for segmenting tumors are now largely dismissed, they can still complement deep neural network architectures. This new thresholding algorithm could serve as a fundamental block of a more complex structure involving deep neural networks for segmentation. Its ability to focus attention on smaller tumor areas could enable deep learning algorithms to concentrate their efforts more effectively.

References

[1] - Louis, D. N., Ohgaki, H., Wiestler, O. D., Cavenee, W. K., Burger, P. C., Jouvet, A., Scheithauer, B. W., & Kleihues, P. (2007). The 2007 WHO classification of tumors of the central nervous system. *Acta Neuropathologica*, *114*(2), 97–109. https://doi.org/10.1007/s00401-007-0243-4

[2] - Liu, J., Li, M., Wang, J., Wu, F., Liu, T., & Pan, Y. (2014). A survey of MRI-based brain tumor segmentation methods. *Tsinghua Science & Technology*, *19*(6), 578–595. https://doi.org/10.1109/tst.2014.6961028

[3] - İlhan, Ü., & İlhan, A. (2017). Brain tumor segmentation based on a new threshold approach. *Procedia Computer Science*, *120*, 580–587. https://doi.org/10.1016/j.procs.2017.11.282

[4] - Aslam, A., Khan, E., & Beg, M. M. S. (2015). Improved edge Detection algorithm for brain tumor segmentation. *Procedia Computer Science*, *58*, 430–437. https://doi.org/10.1016/j.procs.2015.08.057

[5] - Vishnuvarthanan, G., Murugan, P. R., Subbaraj, P., & Vishnuvarthanan, A. (2016). An unsupervised learning method with a clustering approach for tumor identification and tissue segmentation in magnetic resonance brain images. *Applied Soft Computing*, *38*, 190–212. https://doi.org/10.1016/j.asoc.2015.09.016

[6] - Antonelli, M., Reinke, A., Bakas, S., Farahani, K., Kopp-Schneider, A., Landman, B. A., Litjens, G., Menze, B., Ronneberger, O., Summers, R. M., Van Ginneken, B., Bilello, M., Bilic, P., Christ, P. F., Richard, K. G., Gollub, M. J., Heckers, S., Huisman, H., Jarnagin, W. R., . . . Cardoso, M. J. (2022). The Medical Segmentation Decathlon. *Nature Communications*, *13*(1). https://doi.org/10.1038/s41467-022-30695-9

[7] - Wikipedia contributors. (2023, July 23). *Discrete Laplace operator*. Wikipedia. https://en.wikipedia.org/wiki/Discrete_Laplace_operator